



## Crassulacean Acid Metabolism May Alleviate Production of Reactive Oxygen Species in a Facultative CAM Plant, the Common Ice Plant *Mesembryanthemum crystallinum* L.

Haruki Sunagawa, John Cushman & Sakae Agarie

To cite this article: Haruki Sunagawa, John Cushman & Sakae Agarie (2010) Crassulacean Acid Metabolism May Alleviate Production of Reactive Oxygen Species in a Facultative CAM Plant, the Common Ice Plant *Mesembryanthemum crystallinum* L., Plant Production Science, 13:3, 256-260, DOI: [10.1626/tpps.13.256](https://doi.org/10.1626/tpps.13.256)

To link to this article: <https://doi.org/10.1626/tpps.13.256>



© 2010 Crop Science Society of Japan



Published online: 03 Dec 2015.



Submit your article to this journal [↗](#)



Article views: 317



View related articles [↗](#)



Citing articles: 10 View citing articles [↗](#)

[Short Report]

## Crassulacean Acid Metabolism May Alleviate Production of Reactive Oxygen Species in a Facultative CAM Plant, the Common Ice Plant *Mesembryanthemum crystallinum* L.

Haruki Sunagawa<sup>1</sup>, John C. Cushman<sup>2</sup> and Sakae Agarie<sup>1</sup>

<sup>1</sup>Faculty of Agriculture, Saga University, Saga 840-8502, Japan;

<sup>2</sup>Department of Biochemistry and Molecular Biology, University of Nevada, Reno, Nevada 89557-0200 )

**Abstract:** We examined the function of CAM in reactive oxygen species (ROS) alleviation using a newly isolated CAM-deficient mutant of a facultative halophyte *Mesembryanthemum crystallinum* L. Salt-stress (0.4 M NaCl) induced nocturnal malate synthesis in the leaves of the wild-type plant, but not in the mutant. The content of hydrogen peroxide (H<sub>2</sub>O<sub>2</sub>) increased with elapse of time under salt-stress, but it dropped accompanied by the expression of CAM in the wild-type plants. The CAM-performing wild-type plant grown with 0.4 M NaCl for 12 d showed significantly larger diel fluctuation of malate and significantly lower levels of H<sub>2</sub>O<sub>2</sub> than the mutant, particularly at the end of the light period. The transcript abundance of a gene encoding plastidic Cu/Zn-superoxide dismutase (SOD), a marker of ROS production, was higher in the leaves of mutant plants than in those of wild-type plants. These results indicated that the performance of CAM was accompanied by lower levels of ROS and that CAM may help to alleviate oxidative stress under conditions of environmental stress.

**Key words:** CAM deficient mutant, Hydrogen peroxide, *Mesembryanthemum crystallinum* L.

Crassulacean acid metabolism (CAM), one of three modes in the photosynthetic carbon fixation pathway, has been thought to evolve under CO<sub>2</sub>- and water-limiting environments (Silvera et al., 2009). CAM is characterized by nocturnal CO<sub>2</sub> uptake, producing organic acids via the carboxylation of phosphoenolpyruvate (PEP) catalyzed by PEP carboxylase in the dark (Phase I). The organic acids are stored in a large central vacuole (Epimashko et al., 2004) during Phase I accompanied by the glycolytic breakdown of carbohydrates to produce the three-carbon compound, PEP, the substrate for nocturnal carbon dioxide fixation. Decarboxylation of organic acids subsequently occurs during the day and the released CO<sub>2</sub> is refixed by Rubisco behind closed stomata (Phase III). The CO<sub>2</sub>-concentrating strategy in this phase, which can result in a 2-fold to over 60-fold increase results in increased water use efficiency (WUE) in CAM plants, which is several-fold higher than in C<sub>3</sub> and C<sub>4</sub> plants under comparable conditions (Drennan and Nobel, 2000). Thus, CAM is typically associated with plants that inhabit arid environments, semi-arid regions with seasonal water

availability, or habitats with intermittent water supply (e.g. tropical epiphytic habitats) (Cushman and Borland, 2002).

CAM is found in approximately 7% of vascular plant species distributed across 343 genera within 34 families (Holtum et al., 2007) and have been considered to evolve independently multiple times (Silvera et al., 2009). The multiple evolutionary origins of CAM in extreme environments indicate that set of signals common to all environmental stress conditions might be responsible for the adoption of CAM as a metabolic strategy for overcoming water-deficit stress. A key biotic consequence of abiotic stress is the generation of reactive oxygen species (ROS), which can induce a potentially damaging oxidative stress on cellular constituents and/or act as signals for triggering mechanisms of ROS elimination. Two opposite hypotheses in terms of ROS production in CAM plants have been proposed. CAM would prevent the production of ROS during the daytime due to CO<sub>2</sub>-concentration derived from the decarboxylation process, which might reduce over-energization of the photosynthetic machinery under water-limited conditions (Griffiths, 1989). In

contrast, the potential for oxidative stress would increase during the daytime, because the electron transport sustained behind closed stomata and internal O<sub>2</sub> concentrations would be increased substantially (Spalding et al., 1979).

In recent years, investigations into the metabolic, molecular genetic, and signaling elements associated with CAM have employed the facultative CAM species, the common ice plant (*Mesembryanthemum crystallinum* L.). This halophytic species shift its photosynthetic carbon fixation pathway from C<sub>3</sub> to CAM under salt-stress and other abiotic stress factors (Winter and Holtum, 2007; Cushman et al., 2008b). Recently, the function of ROS as key signals for up-regulating the major genes and proteins required for the operation of CAM has been investigated in the common ice plant (Borland et al., 2006; Ślesak et al., 2008). Using recently isolated CAM-deficient mutants of *M. crystallinum* (Cushman et al., 2008a), Borland et al. (2006) investigated the role of ROS in CAM induction in the CAM-deficient mutant and wild-type plants in response to gaseous ozone and salt-stress. The ozone treatment failed to induce functional CAM expression (i.e. net dark CO<sub>2</sub> uptake and nocturnal acidification), but higher CAM expression in wild-type plants induced by salt-stress was accompanied by a potentially lower oxidative load in leaf tissues compared with that detected in the CAM-deficient mutants. ROS was not determined directly but was merely inferred from the increase in the activity of the antioxidant enzyme, superoxide dismutase, at a single time point (Borland et al., 2006).

Here, we demonstrate that CAM induction decreases the oxidative load in wild-type *M. crystallinum* plants relative to CAM-deficient mutants. Our results clearly show that CAM curtailed ROS under salt-stress conditions. Possible mechanisms for CAM-mediated ROS alleviation in *M. crystallinum* are discussed.

### Materials and Methods

Seeds of the wild-type and CAM-deficient mutant (Cushman et al., 2008a) of the common ice plant, *Mesembryanthemum crystallinum* L. were germinated according to the methods described by Sunagawa et al. (2007). Plants were grown hydroponically in a greenhouse under natural sunlight with the temperature oscillating between around 20°C to 30°C and in a growth chamber according to the method described by Agarie et al. (2007). The greenhouse-grown plants were used for measurements of changes in malate and H<sub>2</sub>O<sub>2</sub> with the lapse of time, and the growth chamber-grown plants were used for the measurements of diel changes in contents of malate, H<sub>2</sub>O<sub>2</sub>, and the related elements in the CAM-performing wild-type and CAM-deficient mutant. When plants reached the growth stage at which the 4th leaf appeared (around 40 d after sowing) NaCl was added to the culture solution to a

final concentration of 0.4 M as salt-stress treatment. The leaf tissues were collected from the greenhouse-grown plants at 2, 4, 8, and 16 d after the start of salt-stress treatment at 0700. The leaf tissues were also collected from growth chamber-grown plants every four hours from 0730 to 0330 after 12 d of salt-stress treatment. The excised leaf tissues were immediately frozen in liquid nitrogen and stored at -80°C until use.

Malate contents were measured according to the method described by Chen et al. (2002).

H<sub>2</sub>O<sub>2</sub> content was measured according to the method described by Veljovic-Jovanovic et al. (2002).

Total RNA was extracted by the AGPC (acid guanidinium thiocyanate-phenol-chloroform) method (Chomczynski and Sacchi, 1987).

Semi-quantitative reverse transcription polymerase chain reaction (RT-PCR) was performed using 3 μg total RNA that was reverse-transcribed into first-strand cDNA using the First Strand cDNA synthesis kit (TOYOBO, Japan) according to the manufacturer's instructions. PCR was performed with GoTaq Green Master Mix kit (Promega, USA). After amplification, the reaction products were resolved by electrophoresis on a 1.2% (w/v) agarose gel stained with ethidium bromide. PCR reactions were conducted using 21 cycles. The PCR program was initiated by an initial denaturing step at 95°C for 1 min. RT-PCR conditions were as follows: denaturing at 95°C for 15 s, annealing at 60°C for 30 s, extension at 72°C for 45 s. The program was terminated by a final extension step at 72°C for 7 min. Gel images were captured and quantified by Kodak 1D Image Analysis Software (Kodak, Rochester, USA). Three RT-PCR biological replicates were performed with consistent results. Primers used to generate the amplicons of 402 bp *Sod2* (GenBank, AF034832) and 528 bp *Imt1* (GenBank, M87340) were: forward primer, 5'-TGT CAT CAA TGG CAA CAA CA-3' (T<sub>m</sub>=60°C) and reverse primer, 5'-CCA GCA TTT CCT GTC GTC TT-3' (T<sub>m</sub>=60°C), and forward primer, 5'-ATG AAG TGG GTG TTG CAT GA-3' (T<sub>m</sub>=60°C) and reverse primer, 5'-AAA AAT GCA GCC AGC CTA GA-3' (T<sub>m</sub>=60°C), respectively. Primers used to generate the 435 bp *Ubq* (TIGR, TC7894) amplicon were: forward primer, 5'-TAC TGG AAA GAC TAT CAC CC-3' (T<sub>m</sub>=60°C) and reverse primer, 5'-ATG CCT CCC CTC AAA CGA-3' (T<sub>m</sub>=60°C).

### Results and Discussion

Salt-stress (0.4 M NaCl) resulted in a marked increase in leaf malate content of wild-type plant at the end of dark period (Fig. 1). The induced malate accumulation in leaves was apparent in the wild-type plant after 2 d of salt-stress treatment and increased further by 8 d of salt-stress treatment up to about four-fold compared with non-stressed control plants. In contrast, malate accumulation was induced weakly in the CAM-deficient plants after 16 d

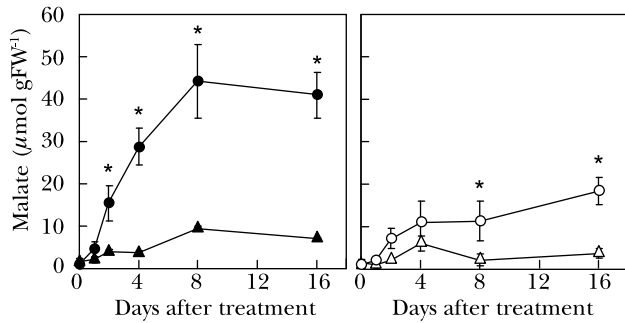


Fig. 1. Changes in malate content of the leaves with lapse of time in wild-type and CAM-deficient mutant plants of *M. crystallinum* after treatment with 0.4 M NaCl. The circle and triangle symbols represent wild-type and mutant plants, respectively. The filled- and open-symbols show the values for the salt- and non-stressed plants, respectively. Values are means of three biological replicates. Each bar shows the standard error. Asterisk indicates statistically significant difference between the wild-type and mutant at each period (Student's t-test,  $p < 0.05$ ).

treatment with 0.4 M NaCl. This was consistent with the results of Cushman et al. (2008a), which showed that day/night fluctuation of titratable acidity was small in the CAM-deficient mutant reflecting only small diel changes in malate content.

In order to determine the effect of CAM induction on ROS accumulation, we monitored the hydrogen peroxide ( $H_2O_2$ ) content during the period of salt-stress treatment.  $H_2O_2$  content of the leaves was higher in the salt-stressed wild-type plants than in the non-stressed plants after 2 d, remained high after 8 d, and then dropped after 16 d of salt-stress treatment to a level similar to that in the non-stressed plants (Fig. 2). In contrast, the CAM-deficient mutant showed a larger increase in  $H_2O_2$  content after 2–8 d of salt-stress treatment that remained elevated (c.a. 80% of maximal) after 16 d of salt-stress treatment. In *M. crystallinum* the induction of CAM expression was generally completed after 10–12 d of salt-stress treatment. The reduction of  $H_2O_2$  accompanied by the expression of CAM, indicating that CAM expression in the wild-type plants was associated with lower levels of  $H_2O_2$ .

After the treatment with 0.4 M NaCl for 12 d, wild-type plants showed a typical CAM rhythm of diurnal malate fluctuation with a 5-fold day/night changes and peak accumulation at dawn (0800) (Fig. 3). In contrast, the CAM-deficient mutant failed to exhibit increased malate accumulation at dawn in leaves under salt-stress with an exception of peak malate accumulation at 1200 up to 10  $\mu$  mol  $gFW^{-1}$ .

The leaves of the salt-stressed CAM performing plants had a lower content of  $H_2O_2$  than the non-stressed wild-type plants during the dark period with the largest differential and the lowest amount occurring at the end of the light period (Fig. 4). The  $H_2O_2$  content ranged from

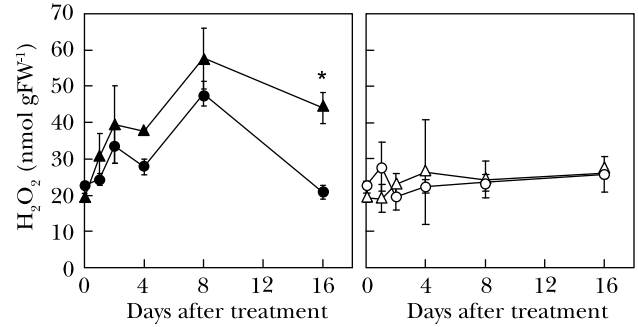


Fig. 2. Changes in hydrogen peroxide content of the leaves with lapse of time in wild-type and CAM-deficient mutant plants of *M. crystallinum* after treatment with 0.4 M NaCl (salt-stressed) or without treatment (non-stressed). The circle and triangle symbols represent wild-type and mutant plants, respectively. The filled- and open-symbols show the values for the salt- and non-stressed plants, respectively. Values are means of three biological replicates. Each bar shows the standard error. Asterisk indicates statistically significant difference between the wild-type and mutant at each period (Student's t-test,  $p < 0.05$ ).

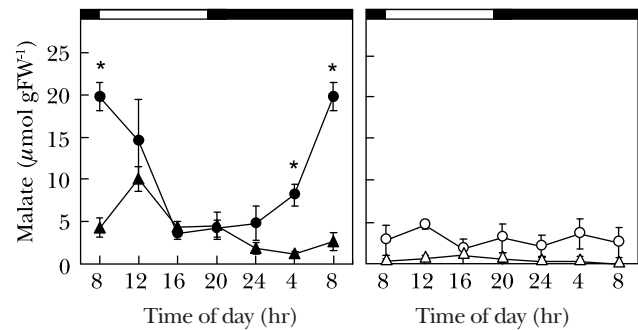


Fig. 3. Diel changes in malate content of the leaves in wild-type and CAM-deficient mutant plants of *M. crystallinum* grown under salt- and non-stressed conditions. The salt-stressed plants were grown with 0.4 M NaCl for 12 d. The circle and triangle symbols represent wild-type and mutant plants, respectively. The filled- and open-symbols show the values for the salt- and non-stressed plants, respectively. Values are means of three biological replicates. Each bar shows the standard error. Asterisks indicate statistically significant difference between the wild-type and mutant at each period (Student's t-test,  $p < 0.05$ ). The horizontal white and black bars on the x axes represent times of light and darkness, respectively.

30–60  $nmol gFW^{-1}$  in the CAM performing plants. In contrast, the content of  $H_2O_2$  of the leaves in the CAM-deficient mutant was higher (60–90  $nmol gFW^{-1}$ ) under salt-stress compared with the wild-type plants and was nearly identical at dusk (2000) between non-stressed and salt-stressed plants.

After 12 d of salt treatment, the wild-type plants grown in the greenhouse (Fig. 1) had a higher malate content at dawn than the CAM-performing wild-type plants grown in the growth chamber (Fig. 3), whereas the  $H_2O_2$  content (Fig. 2) was lower in the former than in the latter (Fig. 4),

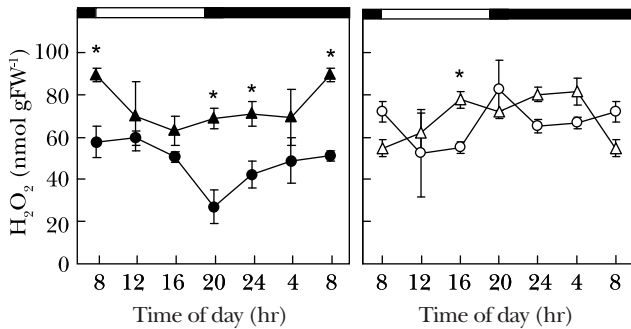


Fig. 4. Diel changes in hydrogen peroxide content of the leaves in wild-type and CAM-deficient mutant plants of *M. crystallinum* grown under salt- and non-stressed conditions. The salt-stressed plants were grown with 0.4 M NaCl for 12 d. The circle and triangle symbols represent wild-type and mutant plants, respectively. The filled- and open-symbols show the values for the salt- and non-stressed plants, respectively. Values are means of three biological replicates. Each bar shows the standard error. Asterisk indicates statistically significant difference between the wild-type and mutant at each period (Student's *t*-test,  $p < 0.05$ ). The horizontal white and black bars on the x axes represent times of light and darkness, respectively.

indicating that in the plant with higher levels of malate (i.e. larger magnitude of CAM expression), the level of  $H_2O_2$  was lower than that in the plant with lower levels of malate.

The induction of CAM in *M. crystallinum* by salt-stress is accompanied by increased activities of the isoforms of SOD such as Mn-SOD, Fe-SOD, and Cu/Zn-SOD, which are found in the mitochondria, chloroplasts, and cytosol, respectively, and the induction of these isoforms of SOD has been used as a marker for ROS production in different subcellular compartments in wild-type and CAM-deficient mutants of *M. crystallinum* (Miszalski et al., 1998; Borland et al., 2006). Borland et al (2006) showed that the activities of the three SOD isoforms in the well-watered leaves collected in the middle of the photoperiod were slightly higher in the CAM-deficient plant than in the wild-type plant, but the salt-stress-induced increase in the activity of all three SOD isoforms was most marked in the CAM-deficient mutant plants. We analyzed the diel changes in the transcript abundance of a cytosolic Cu/Zn-SOD (Fig. 5). The expression levels of the gene for Cu/Zn-SOD was higher in the CAM-deficient mutant than in the wild-type plants, indicating potentially higher oxidative burden in the mutant compared with the wild-type. The transcript abundance of genes responsible for synthesis of radical scavengers (e.g. *Int1*, the gene for myo-inositol *O*-methyltransferase responsible for synthesis of a scavenger, cyclitol) was almost the same between the wild-type and CAM-deficient mutant plants (Fig. 5) and activities of ascorbate peroxidase (APX) and catalase (CAT) were higher in the CAM-deficient mutants than in the wild-type plants (Fig. 6), indicating that the mutant was compensating for the observed ROS load with increased ROS scavenging activities due to its lack of

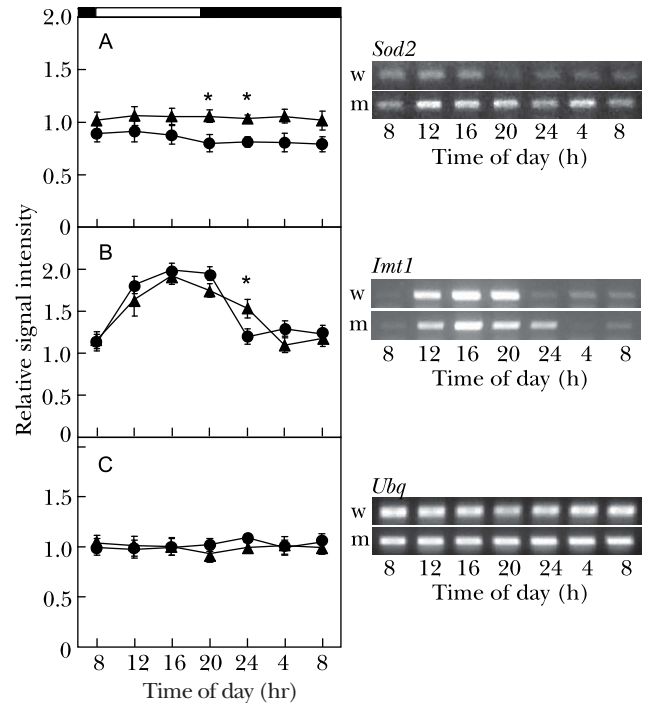


Fig. 5. Diel changes in relative steady-state mRNA abundance of cytosolic CuZn-SOD, myo-inositol *O*-methyltransferase and ubiquitin in the leaves of salt-stressed wild-type and CAM-deficient mutant plants of *M. crystallinum*. The salt-stressed plants were grown with 0.4 M NaCl for 12 d. The circle and triangle symbols represent wild-type and mutant plants, respectively. Values are means of three biological replicates. Each bar shows the standard error. Asterisk indicates statistically significant difference between the wild-type and mutant at each period (Student's *t*-test,  $p < 0.05$ ). w, wild-type; m, CAM-deficient mutant. A: *Sod2*, the gene for cytosolic CuZn-SOD; B: *Int1*, the gene for myo-inositol *O*-methyl transferase; C: *Ubq*, the gene for ubiquitin. The horizontal white and black bars on the x axes represent times of light and darkness, respectively.

functional CAM for alleviation of ROS.

These results clearly show that CAM prevents the production of ROS in the CAM-performing wild-type *M. crystallinum*. The  $CO_2$ -concentration mechanism would contribute to the alleviation of ROS production during the daytime (Griffiths, 1989). However, the lowered  $H_2O_2$  in the salt-stressed CAM performing leaves over the course of the dark period and the lowest levels of ROS occurring at the end of the light period indicate that CAM is associated with another mechanism in the reduction of ROS. We suggest three reasons for decreased ROS in the leaves of salt-stressed CAM-performing wild-type plants. First, the oxidative pentose phosphate pathway (OPPP), which has been shown to control the levels of ROS (Scheibe, 2004) may be associated with lowered ROS in *M. crystallinum*. In *Arabidopsis*, plastidial  $\alpha$ -glucan phosphorylase, which catalyzes the phosphorolysis of the terminal residue from the nonreducing ends of  $\alpha$ -1,4-linked glucan chains, liberating Glc-1-P, has been proposed to play an important

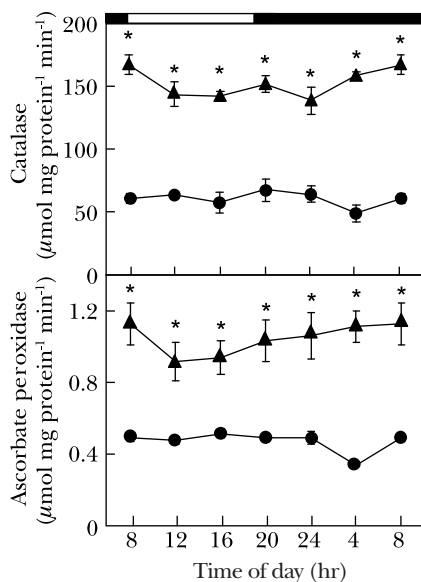


Fig. 6. Diel changes in total activities of CAT and APX in the leaves of salt-stressed wild-type and CAM-deficient mutant plants of *M. crystallinum*. The salt-stressed plants were grown with 0.4 M NaCl for 12 d. The circle and triangle symbols represent wild-type and mutant plants, respectively. Values are means of three biological replicates. Each bar shows the standard error. Asterisk indicates statistically significant difference between the wild-type and mutant at each period (Student's t-test,  $p < 0.05$ ). The horizontal white and black bars on the x axes represent times of light and darkness, respectively.

role in tolerance for salt and drought stresses by providing hexose phosphates as substrates for the OPPP (Zeeman et al., 2004). The OPPP utilizes Glc-6-P, which is crucial for controlling the levels of ROS via the ascorbate-glutathione cycle. The content of hexose-P derived from starch degradation is probably low in the CAM-deficient mutant due to lack of expression of plastidic phosphoglucomutase (PGM), an enzyme critical for gluconeogenesis and starch formation (Cushman et al., 2008a). Second, the alternative oxidase pathway in plant mitochondria, which function in the decrease of formation of ROS generated by the respiratory electron transport (Wagner and Krab, 1995; Maxwell et al., 1999), might be expected to be more fully engaged during the performance of CAM. The 'CAM-related' metabolites such as pyruvate and malate have been shown to activate the key enzyme, alternative oxidase (AOX). Yasui et al. (2004) showed that increased AOX activity measured by the oxygen isotope ( $^{18}\text{O}/^{16}\text{O}$ ) discrimination technique in *M. crystallinum* was accompanied by the transition of photosynthetic mode from  $\text{C}_3$  to CAM, especially during the end of phase I and the beginning of phase II of CAM. Third, ATP utilization in

CAM plants may limit mitochondrial ROS formation by keeping the electron transport chain (ETC) relatively oxidized. In polysaccharide (i.e. starch/glucan)-cycling CAM plants, ATP could be utilized at several points in the CAM pathway, such as in the conversion of starch to hexose-P, hexose-P to triose-P, pyruvate to phosphoenolpyruvate, and 3-phosphoglyceric acid to triose phosphates, and incorporation of malate into the vacuole (Black et al., 1996). The flux through the respiratory mitochondrial ETC and consumption of reducing equivalent in cytochrome pathway would be expected to increase during the transition from  $\text{C}_3$  to CAM in *M. crystallinum*.

In conclusion, our comparative study of the wild-type and a CAM-deficient mutant of *M. crystallinum* showed that the key metabolic elements necessary for operating CAM may serve as part of an overall strategy for alleviating potential ROS damage by increased oxidative load as a consequence of abiotic stresses. The CAM-deficient mutant provides a useful model to further elucidate the effects of anti-oxidant strategies associated with the operation of CAM under a wide range of environmental stress conditions.

## References

- Agarie, S. et al. 2007. *J. Exp. Bot.* 58: 1957-1967.
- Black, C.C. et al. 1996. *In: K. Winter and J.A.C. Smith, eds., Crassulacean Acid Metabolism. Biochemistry, Ecophysiology and Evolution. Ecological studies vol. 114. Springer-Verlag: Berlin.* 31-45.
- Borland, A. et al. 2006. *J. Exp. Bot.* 57: 319-328.
- Chen, L.S. et al. 2002. *J. Exp. Bot.* 53: 341-350.
- Chomczynski, P. and Sacchi, N. 1987. *Anal. Biochem.* 162: 156-159.
- Cushman, J.C. and Borland, A.M. 2002. *Plant Cell Environ.* 25: 295-310.
- Cushman, J.C. et al. 2008a. *Plant Physiol.* 147: 228-238.
- Cushman, J.C. et al. 2008b. *J. Exp. Bot.* 59: 1875-1894.
- Drennan, P.M. and Nobel, P.S. 2000. *Plant Cell Environ.* 23: 767-781.
- Epimashko, S. et al. 2004. *Plant J.* 37: 294-300.
- Griffiths, H. 1989. *In: U. Lüttge, ed., Vascular plants as epiphytes. Berlin: Springer-Verlag:* 42-86.
- Holtum, J.A.M. et al. 2007. *Am. J. Bot.* 94: 1670-1676.
- Maxwell, D.P. et al. 1999. *Proc. Natl. Acad. Sci. USA.* 96: 8271-8276.
- Miszalski, Z. et al. 1998. *Plant Cell Environ.* 21: 169-179.
- Scheibe, R. 2004. *Physiol. Plant.* 120: 21-26.
- Silvera, K. et al. 2009. *Plant Physiol.* 149: 1838-1847.
- Ślesak, I. et al. 2008. *J. Plant Physiol.* 165: 127-137.
- Spalding, M.H. et al. 1979. *Aust. J. Plant Physiol.* 6: 557-567.
- Sunagawa, H. et al. 2007. *Plant Prod. Sci.* 10: 47-56.
- Veljovic-Jovanovic, S. et al. 2002. *Plant Physiol. Biochem.* 40: 501-507.
- Wagner, A.M. and Krab, K. 1995. *Physiol. Plant.* 95: 318-325.
- Winter, K. and Holtum, J.A.M. 2007. *Plant Physiol.* 143: 98-107.
- Yasui, K. et al. 2004. *Jpn. J. Crop Sci.* 73 extra issue 2: 256-257.
- Zeeman, S.C. et al. 2004. *Plant Physiol.* 135: 849-858.